Modelling of detachment in a limiter tokamak as a nonlinear phenomenon caused by impurity radiation

1994 Plasma Phys. Control. Fusion 36 1819

(http://iopscience.iop.org/0741-3335/36/11/009)

Plasma Phys. Control. Fusion 36 (1994) 1819–1843. Printed in the UK

Modelling of detachment in a limiter tokamak as a nonlinear phenomenon caused by impurity radiation

M Z Tokar'†

Institut für Plasmaphysik, Ass. EURATOM-KFA, Forschungszentrum, Jülich, Federal Republic of Germany

Received 6 June 1994, in final form 4 August 1994

Abstract. A numerical one-dimensional radial time-dependent model of particle and energy transport in tokamak plasmas taking the interaction of background and impurity particles through the radiation losses of energy and ion dilution is developed. Detachment in ohmic discharges caused by an increase in the electron density is modelled and the effect of particle and energy transport on detachment conditions is studied. Investigation of dynamic changes in plasma parameters during detachment provoked by an increase in impurity influx is performed. The effect of the nature of heat source on the stabilization of the radiating layer is elucidated. The influence of neo-classical transport and charge-exchange with hydrogen neutrals on the impurity behaviour in 'attached' and 'detached' plasmas is discussed.

1. Introduction

A 'detached' plasma is one of the most spectacular phenomena in tokamaks. In limiter devices it exists as a state with a poloidally symmetric thin shell within the last closed magnetic surface (LCMS), where light impurities radiate almost the total power launched into the discharge (McCracken *et al* 1987, Samm *et al* 1987, Strachan *et al* 1987) (see figure 1). Although it looks like an ideal solution of the problem of the plasma–wall interaction, advantages of a 'detached' plasma for a thermonuclear reactor seem to be questionable. Besides proximity to disruption conditions, it is characterized by degradation in the energy confinement (Weynants *et al* 1988) and by improvement in the confinement of particles (Samm *et al* 1987, Castracane *et al* 1987). For a reactor this would create problems with plasma heating and with exhaust of helium ash.

In order to use radiation from light impurities for cooling of the plasma edge (Samm *et al* 1993) and, nevertheless, avoid a 'detached plasma', one needs to know the conditions under which such states develop. Moreover, 'detachment'—the dynamic process of 'detached plasma' formation—is a brilliant representative of nonlinear phenomena in tokamaks with impurities involved. An investigation of it can give new valuable information on transport processes in thermonuclear devices.

This explains the interest in theoretical studies of detachment and 'detached' plasmas existing for a long time. The complexity of the problem forces one to make different approximations which are not always fulfilled under real experimental conditions. In particular, corona (Post *et al* 1977) or 'enhanced' corona (Neuhauser *et al* 1986) equilibria are often assumed for the distribution of charge states of impurities; convective transport of energy is neglected in comparison with the conductive transport. Moreover, 'typical' profiles

† Permanent address: Institute for High Temperatures, Russian Academy of Sciences, Moscow, Russia.

0741-3335/94/111819+25$19.50

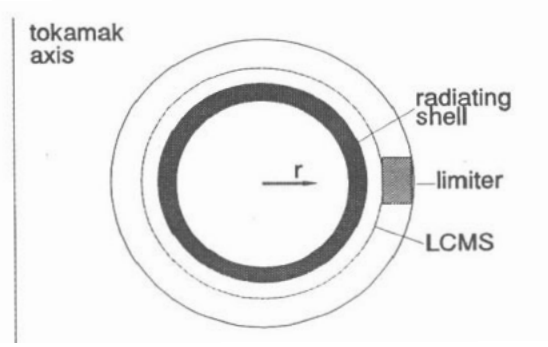

Figure 1. A 'detached' plasma in a tokamak with a toroidal limiter.

of plasma parameters are usually chosen under conditions in which impurity radiation is not of principal importance. On the contrary, observations show that the profiles are modified principally during detachment. As a result, the predictions of models based on the above assumptions (see, for example, Rebut et al 1977, Ohyabu et al 1979, Ashby and Hughes 1981, Behringer *et al* 1986, Krasheninnikov 1988, Tokar' 1989) are in rather crude agreement with the measurements.

The cited failings indicate that states like a 'detached plasma' have to be modelled self-consistently, i.e. with the transport of main and impurity particles and energy taken into account simultaneously. Although certain important effects, for example the influence of impurity motion on radiation losses, allow an analytical interpretation (Tokar' 1994), a firm realization of the foregoing approach can be done only numerically. In the present paper a one-dimensional model of particle and energy transport, realized in the numerical code RITM (radiation from impurities in a transport model) is presented. This model is intended to simulate the effect of radiation on the plasma within the last closed magnetic surface (LCMS); it takes into account the variation of plasma parameters along the minor radius and assumes their homogeneity on the magnetic surfaces.

The structure of the paper is as follows. In section 2 the main assumptions and equations are formulated. In section 3 detachment in ohmic limiter discharges is simulated. The cases of detachment caused by an increase of the plasma density or influx of impurities are investigated and the variation of detachment conditions with transport coefficients is studied. The results of these calculations are compared with experimental data from the tokamak TEXTOR. The role of neo-classical effects and charge-exchange with hydrogen neutrals on transport and on radiation of impurities is considered in section 4. In the appendix certain peculiarities of the model concerning the description of neutrals, ohmic heating and energy losses due to impurities are described.

2. The model for particle and heat transfer in the plasma

2.1. Applicability of a one-dimensional description

The transfer of particles and energy inside the LCMS has at least a two-dimensional character. This is due to the localization of energy sinks and particle sources in the vicinity of the limiter (Allen *et al* 1981, Brau *et al* 1983, Stacey 1987); gas puffing makes the picture still more complicated. However, if the longitudinal transport is sufficiently intensive this

localization does not lead unavoidably to a strong inhomogeneity on magnetic surfaces of such plasma parameters as the electron density n_e and temperature T_e (Tokar' 1992). In particular, the characteristic value of T_e in the maximum radiation is determined mainly by the impurity species (see, for example, Samm 1990). For carbon this is about 30 eV, for neon—about 100 eV. At such a temperature the longitudinal heat conduction is high enough to ensure the homogeneity of T_e. Any significant perturbation of n_e cannot exist either: it would cause plasma motion with a velocity of the order of the ion sound speed and exhaust itself. These qualitative arguments are confirmed by the results of two-dimensional modelling performed by Gerhauser and Claassen (1993).

If the local energy sink becomes too intensive, a strong inhomogeneity of T_e and n_e can arise. For instance, this occurs in the case of gas puffing if the gas influx exceeds a certain critical level (Tokar' 1993). An estimation shows that this level is not achieved under the conditions in question. Moreover, we consider only situations in which a marfe—a poloidally asymmetric cloud of cold, dense and strongly radiating plasma at the inboard side of the discharge (Lipschultz 1987)—does not precede the development of a 'detached' plasma as it was observed in a certain range of discharge parameters in DITE and TEXTOR (McCracken *et al* 1987, Samm *et al* 1987).

Under conditions without strong inhomogeneities in n_e and T_e, the plasma transport equations can be averaged over magnetic surfaces. This is allowed because these equations are linear with respect to quantities that are strong functions of the distance from the limiter. For example, in the continuity equations for impurity ions of low charge, only their densities are such quantities in terms describing sources and sinks due to ionization and recombination.

2.2. *Basic equations*

Averaging results in the following set of one-dimensional equations describing the change of parameters along the minor radius r:
the continuity equations for the background ions

$$\frac{\partial n_i}{\partial t} + \frac{1}{r}\frac{\partial}{\partial r}(r\Gamma_\perp^i) = S_i \tag{1}$$

and for the impurity ions

$$\frac{\partial n_z}{\partial t} + \frac{1}{r}\frac{\partial}{\partial r}(r\Gamma_\perp^z) = k_i^{z-1} n_e n_{z-1} + R_{z+1} n_{z+1} - (k_i^z n_e + R_z) n_z \tag{2}$$

where n_i and n_z are the densities of background and impurity ions of the charge z, respectively; S_i is the source due to ionization of hydrogen neutrals (see appendix 1); k_i^z is the rate coefficient of ionization and R_z is the frequency of electron capture by impurities due to recombination with electrons and charge-exchange with hydrogen neutrals. The densities of charged particles and of their fluxes are related through the plasma quasi-neutrality:

$$n_e = n_i + \sum_z z n_z \qquad \Gamma_\perp^e = \Gamma_\perp^i + \sum_z z\Gamma_\perp^z \tag{3}$$

the equations of the heat balance of electrons

$$\frac{\partial}{\partial t}\left(\frac{3}{2} n_e T_e\right) + \frac{1}{r}\frac{\partial}{\partial r}(r q_\perp^e) = Q_{e,h} + Q_{e,n} + Q_{e,i} + Q_{e,I} \tag{4}$$

and background ions

$$\frac{\partial}{\partial t}\left(\frac{3}{2}n_{\mathrm{i}}T_{\mathrm{i}}\right)+\frac{1}{r}\frac{\partial}{\partial r}(rq_{\perp}^{\mathrm{i}}) \;=\; Q_{i,n}+Q_{i,e} \tag{5}$$

where T_{i} stands for ion temperature; $q_{\perp}^{\mathrm{e,i}}$ are the densities of heat fluxes; $Q_{\mathrm{e,h}}$ is the power density of the ohmic heating (appendix 2), $Q_{\mathrm{e,n}}$, $Q_{\mathrm{i,n}}$ represent the energy transfer in interactions with neutral particles (appendix 1), $Q_{\mathrm{e,i}} = -Q_{\mathrm{i,e}}$ is the energy exchange between electrons and ions owing to Coulomb collisions and $Q_{\mathrm{e,I}}$ are the energy losses from electrons in collisions with impurities due to their ionization, recombination, bremsstrahlung and line radiation (see appendix 3).

The model includes a description of the following neutral particles of the working gas: molecules and reflected atoms coming from the walls, Franck–Condon and hot atoms generated in the plasma by dissociation and charge-exchange. These particles as well as the impurity neutrals are described in the diffusive approximation. The equations governing their densities and fluxes are derived in appendix 1.

The longitudinal electric field $E_{\parallel}$ and current density $j_{\parallel}$ are related to each other through Ohm's law in its simplest form $j_{\parallel} = \sigma_{\parallel}E_{\parallel}$, where $\sigma_{\parallel}$ is calculated by taking neo-classical effects into account (appendix 2). During detachment the total current is maintained unchangeable but $E_{\parallel}$ changes the remaining constant over the plasma cross-section. The latter means that changes in the poloidal magnetic field can occur significantly faster than it is allowed by the classical electro-conductivity. Such behaviour has been observed experimentally on stages of the plasma current ramp up and down (Dnestrovskij *et al* 1979).

In all cases of detachment and 'detached' plasma discussed, the radiating layer is located outside the magnetic surface where the safety factor equals 2. Under such conditions the current profile does not change significantly in the vicinity of this surface and detachment does not provoke a disruption. It is planned to introduce into the model a time-dependent self-consistent MHD consideration to describe more realistically the current evolution during detachment and to treat also the cases with current disruption.

2.3. The transport of charged particles and energy

In the particle flux densities both diffusive and convective components are taken into account:

$$\Gamma_{\perp}^{i,z} = -D_{\perp}^{i,z}\cdot\frac{\partial n_{i,z}}{\partial r}+V_{\perp}^{i,z}n_{i,z}. \tag{6}$$

The anomalous diffusivity $D_{\perp}^{\mathrm{i}}$ and pinch velocity $V_{\perp}^{\mathrm{i}}$ of the background ions are chosen from a comparison of the results of calculations with experimental data because there is still a lack of theoretical background to calculate them self-consistently.

The dependence of the particle confinement time†

$$\tau_p \approx \int_0^a n_{\mathrm{i}}(r)r\,\mathrm{d}r \Big/ \int_0^a S_{\mathrm{i}}(r)r\,\mathrm{d}r \tag{7}$$

† We do not discuss the case of SOL plasmas opaque for neutrals where an essential portion of S_{i} is caused by ionization at $r > a$. This takes place at sufficiently high particle and energy fluxes into the SOL and is not typical for conditions of strong edge radiation.

on such parameters as the mean electron density $\tilde{n}_e$, the plasma current I_p and the input power has been analysed. This gives the possibility to estimate $D_\perp^i$ at the plasma edge (Stangeby and McCracken 1990) in the region where neutrals are ionized, because here the diffusive component in $\Gamma_\perp^i$ overbalances convection.

The analysis, performed for ohmic discharges in TEXTOR, indicates that an Alcator-like scaling

$$D_\perp^i = \frac{A_D}{n_e} \tag{8a}$$

allows us to reproduce the behaviour of τ_p sufficiently well. The value A_D diminishes slightly with increasing plasma current and $A_D \approx 5 \times 10^{16} \mathrm{cm}^{-1}\mathrm{s}^{-1}$ for I_p of 340 kA. In order to avoid a non-adequate strong increase of $D_\perp^i$ as n_e falls approaching the LCMS, the maximal level of diffusivity is restricted by the value equal to 1 $\mathrm{m}^2\,\mathrm{s}^{-1}$ being typical for the SOL.

The relation between the pinch velocity $V_\perp^i$ and $D_\perp^i$ can be found from the density profile in the plasma centre (Strachan *et al* 1982) where $\Gamma_\perp^i \approx 0$. It is close to a parabolic one and

$$V_\perp^i = -\alpha_v \frac{r}{a^2} D_\perp^i \tag{8b}$$

$a_v = 1$ was found as an appropriate fit to reproduce the experimental profile of n_e; in section 3.2 a_v is varied to study the dependence of detachment conditions on the pinch velocity.

The diffusivity of impurity ions is taken equal to that of the background ones: $D_\perp^z \approx D_\perp^i$. At the same time, measurements in TEXTOR (Claassen *et al* 1990, Samm *et al* 1993) show that the convective transport of impurity ions is probably of a different nature than that of deuterons: their total density Σn_z can have a non-monotonous profile whereas the electron density is always peaked at the centre. Such a picture does not contradict the assumption that impurity transfer is governed by the superposition of anomalous diffusion and neo-classical transport. One can distinguish two contributions to the latter. The first 'conventional' component is due to the drifts caused by the toroidal geometry of tokamaks. The second one is caused by poloidal asymmetries of impurity sources (Burrell 1976, Stacey 1987, Claassen and Gerhauser 1992, Stacey 1993). Estimations and calculations (section 4) show that both components are small in comparison with the anomalous transport for the ions of low z localized at the plasma edge and making the greatest contribution to radiation. This is due to very sharp gradients of the densities of these ions caused by ionization into the next charge states. In the central plasma the source asymmetry is not pronounced and for strongly ionized impurities we take into account only 'conventional' neo-classical transport with the radial fluxes calculated according to Wenzel and Sigmar (1990). We plan to introduce into the model the recent developments in the transport theory (Stacey 1993, Rogister 1994) and to take into account the effect of plasma rotation (Groebner *et al* 1990, Ida *et al* 1994).

The heat fluxes transferred by ions and electrons have components of conductive and of convective nature:

$$q_\perp^{e,i} = -\kappa_\perp^{e,i} \cdot \frac{\partial T_{e,i}}{\partial r} + \frac{5}{2} \Gamma_\perp^{e,i} T_{e,i}. \tag{9}$$

An Alcator-like scaling and a neo-classical coefficient are used for electron and for ion heat conductivities, respectively:

$$\kappa_\perp^e = 3\alpha_\kappa A_D \qquad \kappa_\perp^i = \kappa_i^{neo}. \tag{10}$$

The coefficient a_k is taken equal to 1 in section 3.1; it is varied in section 3.2 to study the effect of the conductive heat transport on the detachment conditions; κ_i^{neo} is calculated according to the formulae of Hinton and Hazeltine (1976).

2.4. Boundary conditions

At the discharge axis ($r = 0$) derivatives of all variables reduce to zero. At the LCMS ($r = a$) the e-folding lengths of the densities and temperatures are prescribed:

$$\frac{\partial n_{i,z}}{\partial r} = -\frac{n_{i,z}}{\delta_n^{i,z}} \qquad \frac{\partial T_{e,i}}{\partial r} = -\frac{T_{e,i}}{\delta_T^{e,i}}. \tag{11}$$

They are governed by the transport in the SOL. In the present study we take $d_{n,T}$ from experimental data (Samm *et al* 1987, Samm U *et al* 1989a).

In the consideration of stationary states the influx of the hydrogen neutrals through the LCMS ,is determined by the condition of total recycling (see appendix 1); in the non-stationary case of detachment it is defined using the requirement to have a prescribed average density of electrons. The influxes of neutrals of carbon and oxygen are related to the outflow of background ions through the effective erosion coefficients $a_{C,O}$. The values of these are assumed to be constant. This assumption is justified to a certain extent by the experimental data (Bogen and Rusbüldt 1992); in particular, a decrease of physical sputtering with the reduction of the edge temperature during detachment is compensated for by an increase in chemical erosion, probably due to the drop of the limiter temperature (the rate of chemical erosion has a maximum at a surface temperature of several hundred K).

3. Results of calculations

3.1. Detachment due to a change in plasma density and current

An increase of the electron density is a well known cause of detachment. It develops abruptly as the mean density $\tilde{n}_e$ exceeds a certain critical value. For a fixed $\tilde{n}_e$ a detachment may be provoked by a reduction of the plasma current I_p. The findings on different devices (Lipschultz 1987, Samm *et al* 1987) show that in both cases the onset of detachment occurs at roughly the same magnitude of the parameter $\rho = \pi a^2 \tilde{n}_e / I_p$. In machines with carbonized walls this critical level lies in a range of $4\text{–}7 \times 10^{11}$ A^{-1} cm^{-1}†. As an example detachment caused by the increase of n_e in ohmic discharges in TEXTOR with carbonized walls and $a = 46$ cm, $R = 175$ cm, $B_T = 2.25$ T is simulated. For the relative inflows of carbon and oxygen atoms the magnitudes typical for these conditions are taken as: $a_C = 0.03$, $a_O = 0.01$ (Samm *et al* 1987, Unterberg *et al* 1993); $A_D = 5 \times 10^{16}$ cm^{-1}s^{-1} and $\kappa_\perp^e = 1.5 \times 10^{17}$ cm^{-1}s^{-1} are used for transport coefficients; $d_n^{i,z} = 1$ cm, $d_T^e = 2$ cm and $d_T^i = 3$ cm—for the decay lengths at the LCMS.

Figure 2 shows the radial profiles of the power density Q_{rad} of impurity radiation and of the electron temperature, calculated for different magnitudes of n_e and $I_p = 340$ kA. The onset of a 'detached plasma' occurs as n_e exceeds a critical value of 3.6×10^{13} cm^{-3}: the maximum of radiation displaces towards the discharge centre and the electron temperature falls at the LCMS from 12 eV at $n_e = 3.3 \times 10^{13}$ cm^{-3} to 3 eV at $n_e = 3.8 \times 10^{13}$ cm^{-3}.

Inward displacement of the radiating layer in a 'detached' plasma is accompanied by a significant increase of the maximum of Q_{rad}. This is caused mainly by two factors. First, the density of the impurity increases because the confinement time of the impurity ions becomes larger due to a deeper penetration of neutrals into the plasma with decreasing edge temperature. This is demonstrated in figure 3, where the density profiles of different carbon

† Note that the detachment condition is close to the Hugill density limit (Greenwald *et al* 1988) which can be written as $\rho = \kappa \times 10^{12}$ A^{-1} cm^{-1}, where κ is the plasma elongation.

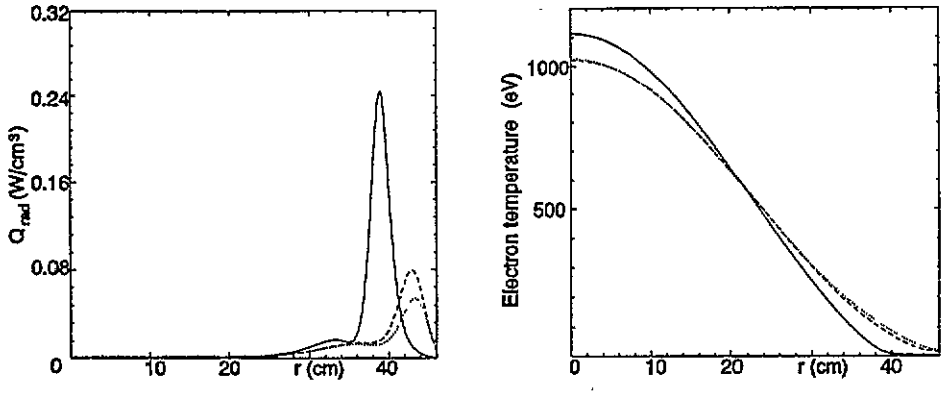

Figure 2. The profiles of Q_{rad} and T_e for different n_e: points—2.8×10^{13} cm^{-3}, dashed lines—3.3×10^{13} cm^{-3} and solid lines—3.8×10^{13} cm^{-3}.

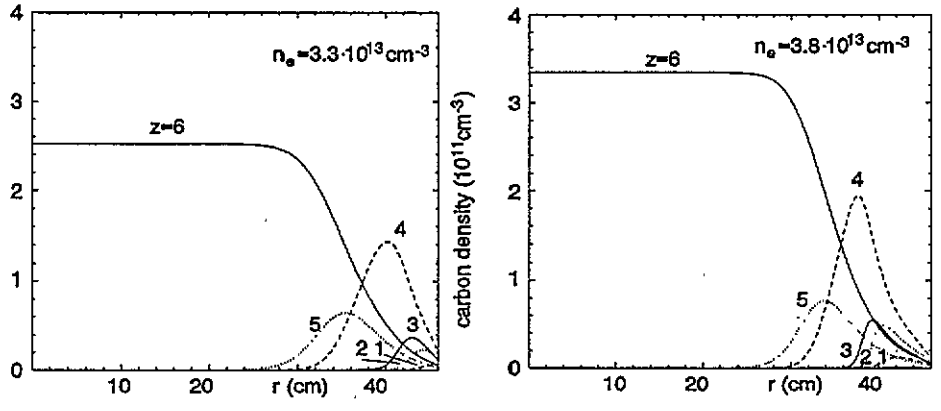

Figure 3. The radial profiles of the carbon ion density.

ions are shown for an 'attached' plasma with $\tilde{n}_e = 3.3 \times 10^{13}$ cm^{-3} and for a 'detached' one with $\tilde{n}_e = 3.8 \times 10^{13}$ cm^{-3}. Second, Li-like carbon impurities, making the main contribution to radiation (figure 4), hit the region of a larger electron density where they are excited more often. The corresponding radial profiles of n_e are presented in figure 5.

In addition to a steepening of the n_e profile at the position of the main radiation, a 'detached' plasma is characterized by a noticeable decrease of n_e at the LCMS and in its vicinity. Similar to the case of impurities, this drop in $n_e(a)$ is also caused by an increase in the penetration depth l_n of neutrals, in particular, when T_e at the edge becomes less than the ionization potential of hydrogen. This is illustrated in figure 6, where the profiles of the source density S_i of deuterons are shown. As a result the plasma outflow through the LCMS drops. One can see this from the simple estimate $\Gamma^i_\perp(a) \approx D^i_\perp \tilde{n}_e / l_n$ (Stangeby and McCracken 1990). According to the boundary condition (11) the density at the LCMS changes proportionally to $\Gamma^i_\perp(a)\delta^i_n$. Although in reality δ^i_n also changes with the temperature at the LCMS, this alteration is much weaker than that of $\Gamma^i_\perp(a)$.

The reduction of the particle loss through the LCMS explains a drastic increase in the confinement time $\tau_p \sim \tilde{n}_e / \Gamma^i_\perp(a)$ observed after detachment (Samm *et al* 1987, Castracane

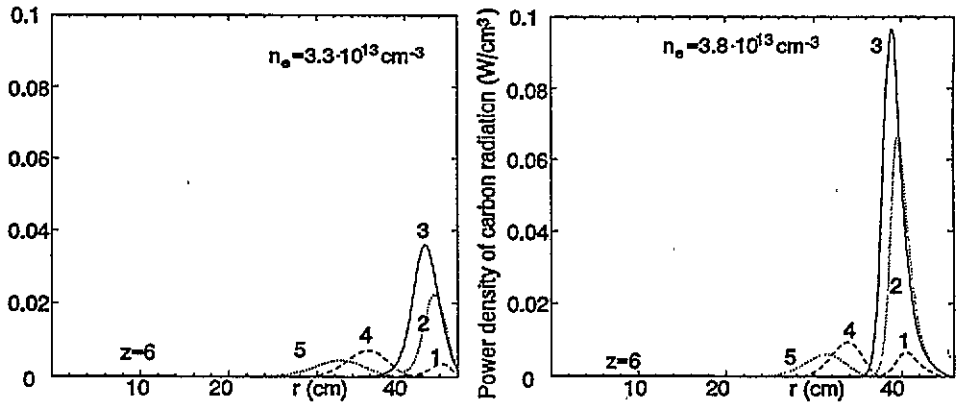

Figure 4. The radial profiles of the power density of carbon radiation (bremsstrahlung from fully ionized particles is negligibly small).

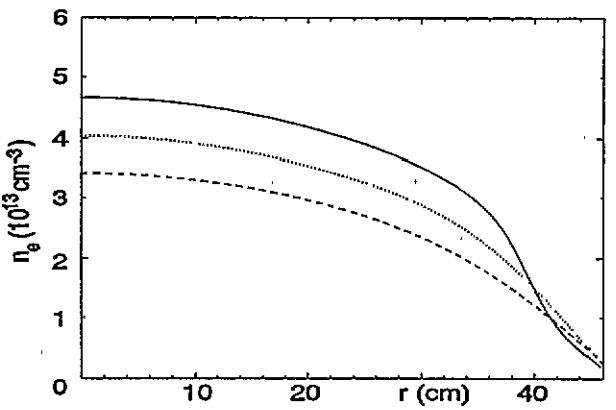

Figure 5. The radial profiles of electron density for different $\tilde{n}_e$: dashed line—2.8×10^{13} cm^{-3}, points—3.3×10^{13} cm^{-3} and solid line—3.8×10^{13} cm^{-3}.

et al 1987). The displacement of the S_i maximum to the centre correlates with the behaviour of the measured H_α radiation from hydrogen atoms (Samm *et al* 1989b).

The radiation level γ_{rad}—the ratio of the power radiated by impurities to the input power—is shown in figure 7 against the mean electron density. In the vicinity of the onset of detachment ($\tilde{n}_e \approx 3.6 \times 10^{13}$ cm^{-3}) the strong nonlinear increase of γ_{rad} with $\tilde{n}_e$ is evident. This is caused by the factors stressed above: by penetration of the radiating ions into the region of higher electron density and by an increase of the impurity confinement time. By neglecting these nonlinear properties, the modelling of impurity radiation can result in large discrepancies with experiments (Samm *et al* 1990). The model calculation of γ_{rad} are in a good agreement with experimental data (Samm *et al* 1990) which are also shown in figure 7. In a 'detached plasma' 10–15% of the input power is lost by the hydrogen radiation and neutrals. These channels are not included in the foregoing definition of the radiation level. Therefore, the theoretical value of γ_{rad} saturates at 0.85, although the energy losses to the limiter are essentially less than a $(1 - \gamma_{rad})$ fraction of the power launched.

The plasma density at which the detachment occurs in the reference case of $I_p = 340$ kA

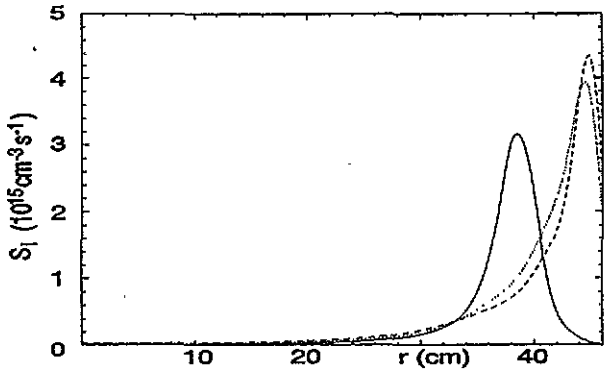

Figure 6. The source density of background ions: dashed line—$\bar{n}_e = 2.8 \times 10^{13}$ cm^{-3}, points—3.3×10^{13} cm^{-3} and solid line—3.8×10^{13} cm^{-3} (a 'detached' plasma).

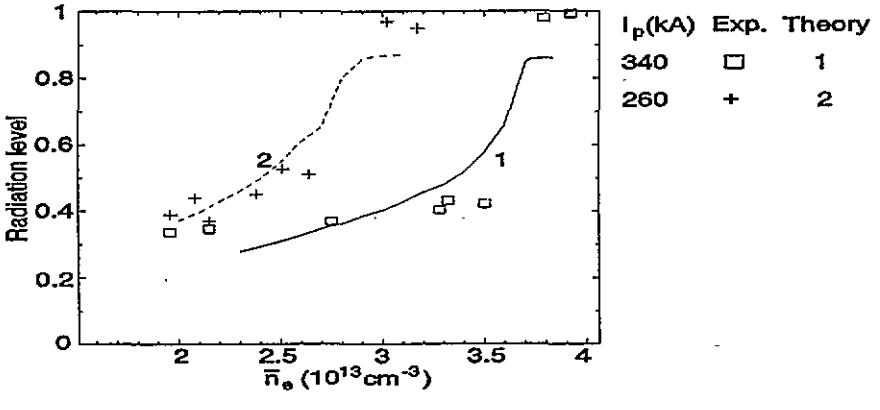

Figure 7. The experimental (symbols) and calculated (curves) dependences of the radiation level on the mean plasma density for different magnitudes of the plasma current.

(curve 1 in figure 7), corresponds to the critical parameter $\rho \approx 7 \times 10^{11}$ A^{-1} cm^{-1}. A similar value of ρ follows for the case of $I_p = 260$ kA presented by the curve 2 in figure 7.

3.2. Effect of particle and heat transport on the detachment conditions

Changes in the transport of charged particles and energy results in an alteration of the detachment conditions. This has been demonstrated, e.g. by Vallet *et al* (1991) in Tore Supra, where an 'attached' plasma has been resumed from a 'detached' one by activation of the ergodic divertor (ED) or in auxiliary heated discharges in TEXTOR with neon puffing where 'attached' plasmas have been realized at γ_{rad} close to 100% (Samm *et al* 1992a, Samm *et al* 1992b).

Here we analyse the effect of a change in the magnitudes of transport coefficients. The calculations are done for ohmic TEXTOR plasmas with $I_p = 340$ kA, $a_C = 0.03$ and $a_O = 0.01$. Figure 8 presents the density dependence of the radiation level found for different combinations of the parameters A_D, a_V and a_k, which represent the particle diffusivity, pinch

velocity and anomalous heat conductivity respectively. Curve 1 corresponds to the reference case studied in the previous section (the same as curve 1 in figure 7).

Particle diffusivity. An increase in the particle diffusivity by a factor of 2 (curve 2 in figure 8) leads to a higher radiation level at a given density. This is caused by the increase in the deuteron outflow to the LCMS, proportional to $D_\perp^i$. As a result the convective loss of energy rises and the edge temperature reduces, thereby leading to an increase of the radiation. At the same time the plasma becomes more stable to detachment; i.e. the radiating layer remains in the vicinity of the LCMS until γ_{rad} exceeds about 0.75. An analysis (Tokar' 1994) indicates that this effect is caused primarily by the change in impurity transfer. If the diffusivity is increased for the background ions only the radiation level, at which the onset of detachment occurs, reduces.

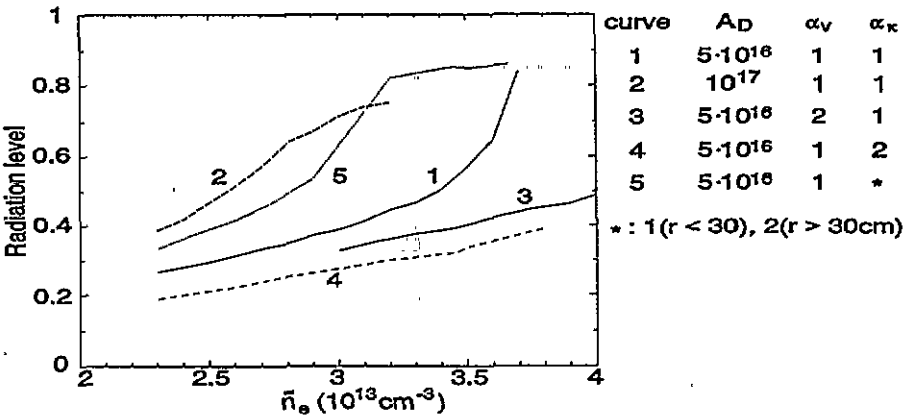

Figure 8. The density dependence of the radiation level for different combinations of parameters characterizing the transport of particles and energy.

Pinch velocity. Curve 3 in figure 8 corresponds to the pinch velocity increased by a factor of 2 with respect to the reference case. This leads to a peaking of the plasma density profile. For a given $\bar{n}_e$, the edge density and the particle outflow through the LCMS decrease. As a consequence, the convective loss of energy decreases, the edge temperature becomes higher and the radiation reduces. As a result, the plasma can change over from detached to attached. For the case under consideration, the radiation level does not exceed 50% for mean electron density less than 4×10^{13} cm^{-3}.

Electron heat conductivity. An increase of $\kappa_\perp^e$ in the whole discharge (curve 4) also results in a decrease of the radiation level. This can be understood as follows. If radiation does not dominate in the heat balance the edge temperature is determined by the power, transported from the core conductively and lost with particles to the limiter. By increasing $\kappa_\perp^e$ in the entire discharge one decreases the averaged electron temperature and the ohmic power grows. At the same time the particle loss changes weakly. Thus the edge temperature increases and radiation becomes still less important. An opposite situation takes place if $\kappa_\perp^e$ becomes larger only at the plasma edge (curve 5). In this case γ_{rad} increases with the plasma density more pronouncedly than for the reference heat conductivity.

At first sight the latter behaviour contradicts the changes in the radiation pattern observed in Tore Supra during activation of ED (Vallet 1991). There the plasma heat conductivity was increased at the edge by stochastization of the magnetic field and simultaneously an 'attached' plasma has been resumed from a 'detached' one. This contradiction vanishes if we

take into account that not only magnitude but also the temperature dependence of $\kappa_\perp^e$ has been altered. In a stochastic field the heat transport along lines of force contributes significantly to the effective transport across unperturbed magnetic surfaces and $\kappa_\perp \sim k_\parallel \sim T_e^{5/2}$ (see e.g. Yamagishi *et al* 1983). A stronger temperature dependence of $\kappa_\perp$ makes the plasma more stable to detachment which can be understood qualitatively as follows.

Varying the discharge conditions we change the plasma temperature at the LCMS which is determined by the balance between the input power and the energy losses from the discharge. As a function of $T_e(a)$, the latter can have a minimum since the losses with particles increase and those with radiation decrease with increasing $T_e(a)$ (Tokar' 1994). This occurs because in 'attached' plasmas radiation is emitted from the layer where electron temperature changes between $T_e(a)$ and a certain value close to half the ionization potentials of Be- and Li-like impurity ions (see section 3.1 of this paper, Samm *et al* 1990, Tokar 1994). As $T_e(a)$ decreases, this layer becomes wider. Detachment occurs as the input power becomes less than the minimal losses.

A stronger temperature dependence of $\kappa_\perp^e$ results in a more convex temperature profile and the width of the radiating layer becomes less sensitive to the magnitude of $T_e(a)$. As a result, the minimum of energy losses can vanish so that the plasma remains attached at a high radiation level. These arguments are confirmed by the results of calculations done with $\kappa_\perp^e$ enhanced as follows at the edge with respect to the reference case: $\kappa_\perp^e(r > 30\,\text{cm}) = 1.5 \times 10^{17}\ \text{cm}^{-1}\text{s}^{-1} + \zeta_k T_e^{5/2}$, where ζ_k is chosen so that the mean value of $\kappa_\perp^e$ in the region $30 < r < 46$ cm is equal to $3 \times 10^{17}\ \text{cm}^{-1}\text{s}^{-1}$. Calculations give that in this case the plasma does not detach for a radiation level lower than 0.85.

Note that a stronger temperature dependence of the particle diffusivity also results in an enhanced stability to detachment (Tokar' 1994).

e-folding lengths at the LCMS. These lengths, applied as boundary conditions, change significantly during detachment (Samm *et al* 1987). For instance δ_n increases by a factor of 2–3. At the same time calculations performed with $\delta_{n,T}$ increased by the same factors with respect to the values used previously have shown a very weak effect of these changes on the detachment conditions: the critical values of the plasma density and radiation level change by less than 10%. This becomes understandable if we assume that the modifications in the scrape-off layer are not causes but consequences of detachment caused by the decrease of the energy outflow to the SOL. To better investigate this question we plan to couple the present model to a self-consistent description of the SOL plasma.

3.3. Dynamics of a detachment

In order to simulate how a 'detached' plasma arises we consider a detachment provoked by an increase in the impurity flux into the plasma. This may occur, for instance, with injection of impurities, with appearance of hot spots (Ulrickson *et al* 1990) or with plasma polarization by electrodes (Van Nieuwenhove *et al* 1992).

As an initial state we take an 'attached' ohmic plasma in TEXTOR with $I_p = 340$ kA, $\tilde{n}_e = 3.5 \times 10^{13}\ \text{cm}^{-3}$, $a_C = 0.024$ and $a_O = 0.008$. At $t = 0$ the relative impurity influxes are increased by a factor of 2. Figure 9 shows the evolution of Q_{rad} and T_e profiles in time. Detachment occurs in the form of a cooling pulse propagating from the edge into the plasma. The sequence of events is as follows. An initial increase of the radiation due to the enhanced influx of impurities leads to a certain plasma cooling and impurity particles of low z penetrate more deeply into the plasma. As a result Be- and Li-like ions, which make the main contribution to the radiation, are produced in the region of a higher electron density. The density of impurity ions also grows due to better particle confinement. Thus the power

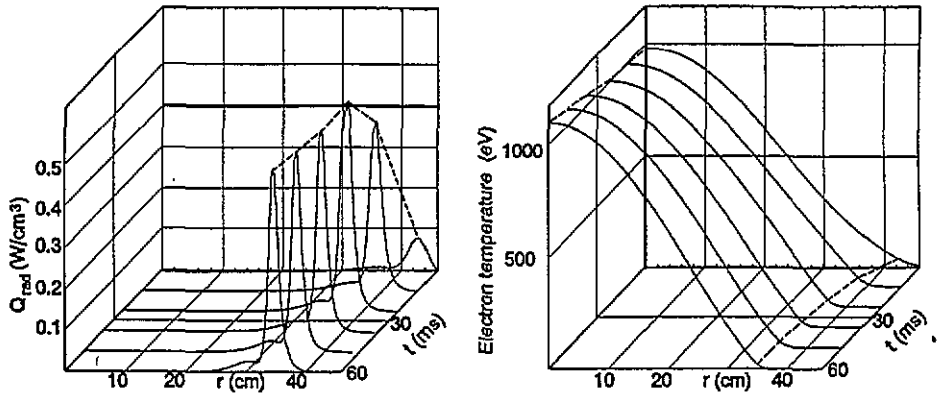

Figure 9. Time evolution of the power density Q_{rad} of impurity radiation and of the electron temperature during the detachment.

density of radiation increases further. The local energy losses cannot be compensated by the heat flux from the plasma core and the radiating layer moves inward.

As can be seen in figure 9, the detachment occurs during a characteristic time of 10–20 ms, which is in agreement with experimental observations (Van Nieuwenhove *et al* 1992).

What prevents thermal collapse? The approach to the asymptotic state of a 'detached' plasma is manifested (figure 9) in the slowing down of the cooling wave. Why does the radiating layer not move further towards the discharge centre? The cause for this stabilization lies in the nature of the heat source. With *ohmic heating* the model can very well explain this stabilization. The modification of the electron temperature profile leads to a change in the power density profile: as T_e and the plasma electro-conductivity reduce at the edge, the current profile becomes more peaked, the plasma inductance increases, the longitudinal electric field grows and ohmic dissipation increases in the discharge centre. As a result, the density of the heat flow to the periphery increases and a 'thermal barrier' arises, which stops the motion of the radiating layer towards the centre. This is demonstrated in figure 10, where the time evolution of the radial profiles of the density of the heat source and of the electron heat flux is shown for the conditions described in the previous section.

Thus in ohmic discharges the redistribution of the heat source during detachment plays a decisive role in the formation of a quasi-stationary 'detached plasma'. If the heat source has a different nature and such a redistribution does not take place, the radiating layer can penetrate to the discharge centre and results in a thermal collapse of the plasma column. This is demonstrated in figure 11 by the time evolution of T_e and Q_{rad} profiles, calculated for the same conditions as the profiles in figure 9,10 but with the heat source density homogeneous over the plasma volume and independent of parameters: $Q_{e,h}(r) = 0.04$ W/cm^3. This magnitude is chosen from the requirement to have approximately the same input power as in the case of ohmic heating. The behaviour found is similar to the thermal collapse in current-free plasmas, e.g. in the torsatron ATF by neon puffing (Hiroe *et al* 1992).

A consideration of detachment in auxiliary heated plasmas in tokamaks is beyond the scope of the present paper. But it is important to note that additional heating usually results in a change of the particle and energy transport. This can lead to an alteration both of

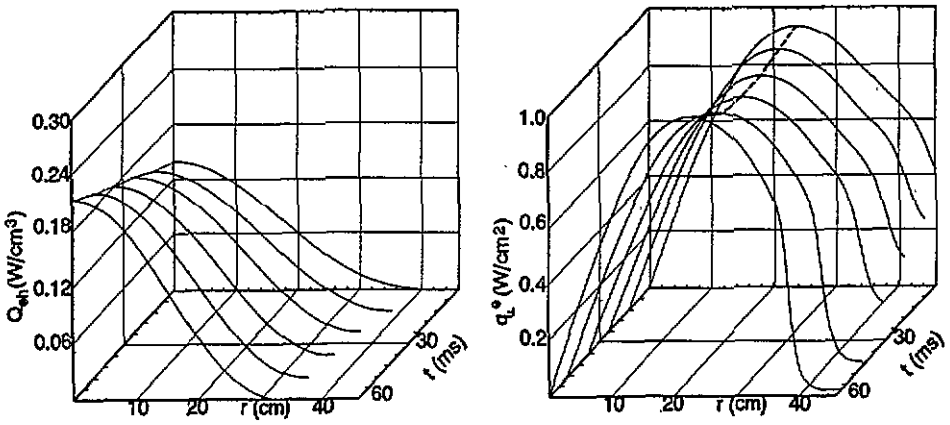

Figure 10. The time evolution of the densities of the heat source and of the electron heat flux during the detachment.

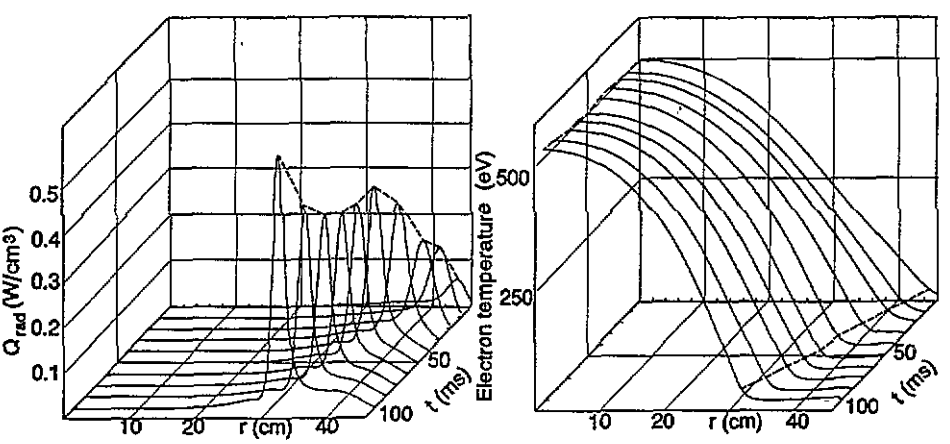

Figure 11. Time evolution of the power density of radiation and of the electron temperature during a thermal collapse in a plasma with non-ohmic heating.

the detachment conditions (see 3.2 and Tokar' 1994) and of the mechanism of detachment stabilization.

4. The role of neo-classical effects and of charge-exchange with hydrogen neutrals in impurity transport and radiation

The transport of impurity particles significantly influences the radiation losses. The results

of the foregoing consideration, taking into account the anomalous diffusion, ionization and radiative recombination of impurities, agree well with the measurement data. Here we consider the effect of neo-classical transport and of charge-exchange with hydrogen atoms which are often discussed as factors being very important for the impurity behaviour. It is shown that this effect is not principal for ions of low charge which are responsible for radiation. Conversely, it is essential for fully stripped ions, especially in a 'detached' plasma, which determine the level of plasma pollution.

4.1. Neo-classical transport

Neo-classical transport is often discussed as a cause of impurity accumulation in tokamak discharges because the neo-classical convection driven by the gradients of n_i and T_i can be directed toward the plasma centre. According to Wenzel and Sigmar (1990), the velocity of this convection can be written as follows ($z \gg 1$ is assumed):

$$V_\perp^z = \frac{q^2\rho_i^2}{\tau_{ii}} z \left(\frac{K}{n_i}\frac{\partial n_i}{\partial r} + \frac{H}{T_i}\frac{\partial T_i}{\partial r} \right) \tag{12}$$

where ρ_i is the gyro-radius of background ions and τ_{ii} is the time between their mutual Coulomb collisions. The coefficients K and H depend on the collisionalities g_i and g_z of the main and impurity particles. The collisionalities are defined as the ratio of the proper collisional frequency and the bounce frequency of the motion on banana orbits. In the case of impurity ions of the charge z, mass m_z and density n_z we have:

$$g_z = \frac{4\sqrt{\pi}}{3}\frac{e^4 R q \ln\Lambda n_e}{T_i^2} z^2 \varphi_z$$

where R is the major radius, $\ln\Lambda$ is the Coulomb logarithm,

$$\varphi_z = z_{\text{eff}} - 1 + \sqrt{\frac{m_i}{m_z}} + z\left(1 - \sqrt{\frac{m_i}{m_z}} - 0.293z\right)\frac{n_z}{n_e}$$

and $z_{\text{eff}} = (n_i + \Sigma z^2 n_z)/n_e$ is the effective charge of the plasma.

Radiating impurity ions. Impurity ions whose charge is less than that of the He-like ones, are localized at the plasma edge. The characteristic length of their density variation is significantly less than those of n_i and T_i which determine the neo-classical convection. Therefore, the contribution to the flux density from anomalous diffusion, being proportional to the gradient of n_z, is predominant for these particles. Since they are of maximum importance for the radiation losses, the diffusive approximation with $V_\perp^z = 0$ is justified for calculation of radiation.

Fully stripped ions. For these particles the situation is different. Their source is negligible in the main part of the plasma and neo-classical convection has to be balanced by anomalous diffusion. Thus the density profile cannot be flat, as predicted by the diffusive approximation (figure 3). Figure 12 shows the profiles of the collisionalities of the background ions and carbon nuclei calculated for an 'attached' plasma with $\tilde{n}_e = 3.3 \times 10^{13}$ cm^{-3}, $I_p = 340$ kA, $a_C = 0.03$ and $a_O = 0.01$. In the outer region $25 < r < 46$ cm we find $g_z > 1$, so that the impurity is in the Pfirsch–Schlüter (PS) transport regime. In this case the coefficients K and H depend on the collisionality g_i of the background ions and on the value $a_z = n_z z^2/n_i$ as follows (Wenzel and Sigmar 1990):

$$K = 1 - \frac{0.52\alpha_z}{0.59 + \alpha_z + 1.34 g_i^{-2}} \qquad H = -0.5 + \frac{0.29 + 0.68\alpha_z}{0.59 + \alpha_z + 1.34 g_i^{-2}}. \tag{13}$$

For typical $n_z/n_i \approx 0.01$, $a_z \approx 0.35$, one can distinguish two sub-regions: (*a*) $39 < r < 46$ cm where $g_i > 3$, K≈ 0.8, $H > 0$ and both components of the neo-classical convection due to the gradients of the density and temperature of the background ions are directed towards the plasma centre; (*b*) $25 < r < 39$ cm where $K \approx 0.8$–1, $H < 0$ and the component due to $\partial T_i/\partial r$ is directed outward—a so-called temperature screening takes place.

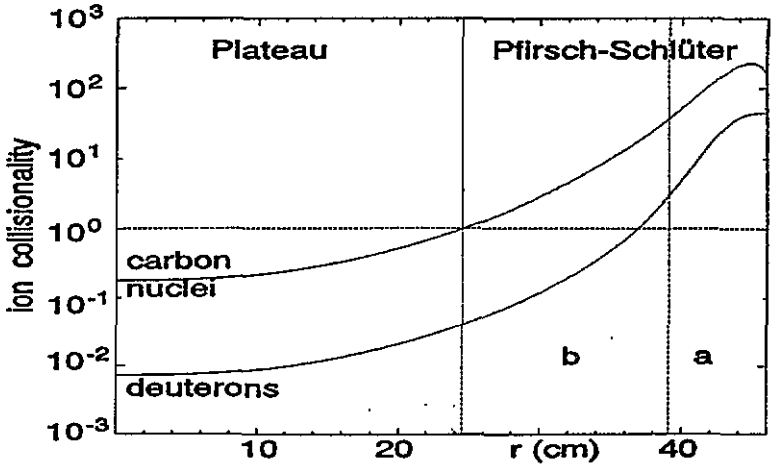

Figure 12. The radial profiles of collisionalities of deuterons and carbon nuclei (the used profiles of plasma parameters are presented in figures 2 and 5).

In the inner plasma region $0 < r < 25$ cm the inequality $(r/R)^{3/2} < g_z < 1$ holds and the impurity is in the plateau regime of neo-classical transport. In this case using the results of Wenzel and Sigmar (1990) we obtain $K \approx g_z^{-1}$ and $H \approx g_z^{-1}\zeta$, where $\zeta \approx 1.5$ for $(r/R)^{3/2} \ll g_i$ and $\zeta \approx -0.173$ in the opposite limit; in the calculations the dependence on g_i is approximated as $\zeta = 1.5 - 1.673\exp(-g_i(R/r)^{3/2})$.

Thus the structure of the neo-classical flux is complicated and regions, where $V_\perp^z$ is directed inward, may alternate with those where the direction is opposite. This is demonstrated in figure 13, where the profiles of the flux components of carbon nuclei due to anomalous diffusion Γ_{an} and due to neo-classical convection Γ_{neo} are shown; the contributions $\Gamma_{neo}^{\nabla n}$ and $\Gamma_{neo}^{\nabla T}$ to the latter, driven by the gradients of n_i and T_i, respectively, are also presented.

Figure 14 shows the density profiles of carbon nuclei computed for the above case of an 'attached' plasma in (*a*) the diffusive approximation ($V_\perp^z = 0$) and (*b*) taking the neo-classical transport into account. One sees that the net effect of the neo-classical transport is the accumulation of C^{+6} ions in the centre. Experimental observations show that under these conditions $z_{eff} \approx 1.5$ in the plasma centre (Hintz 1992). This corresponds to $n_6 \approx 7 \times 10^{11}$ cm^{-3} which is in good agreement with calculations carried out with neo-classical effects. Also measurements of C^{+6} density by charge-exchange spectroscopy employing a Li beam (Schorn *et al* 1991) give values which are in the range of the calculated ones.

In a 'detached' plasma the role of neo-classical transport becomes even more important. The velocity of convection increases at the plasma edge since in the PS regime $V_\perp^z \sim T_i^{-1/2}$.

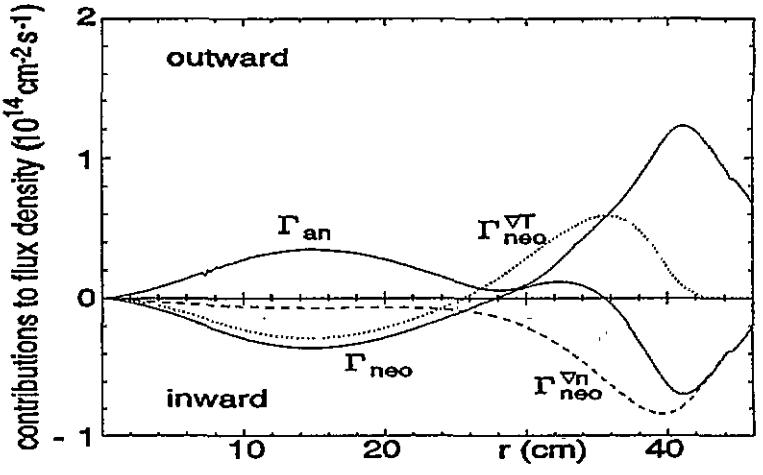

Figure 13. The contributions to the flux density of carbon nuclei due to anomalous diffusion and neo-classical convection.

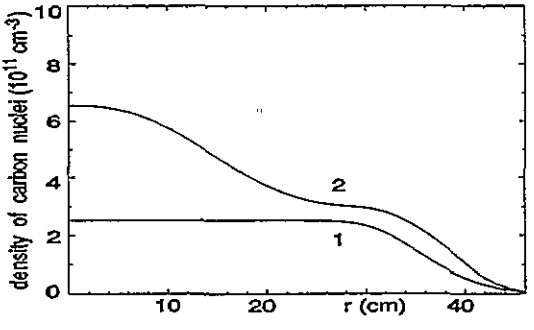

Figure 14. The radial profiles of the carbon nuclei density in an 'attached' plasma calculated in the diffusive approximation (1) and taking into account the neo-classical convection (2).

The temperature profile is flat here and the component of the impurity flux due to the gradient of n_i is predominant. It is directed to the centre and may lead to a strong accumulation of impurities, so that z_{eff} can reach a value of 3. Such a pollution of TEXTOR plasmas by low-z impurities was never observed experimentally; there are probably other mechanisms expelling impurities. A possible candidate can be charge-exchange (CX) of impurities with hydrogen neutrals discussed in the following section.

4.2. Charge-exchange of impurities with hydrogen neutrals

Charge-exchange (CX) with hydrogen neutrals reduces the charge of impurity ions and generates, in particular, strongly radiating Li-like particles from He-like ones. This effect was discussed previously (Tokar' 1988, Abramov *et al* 1992) as a likely trigger of radiative instabilities and detachment.

In an 'attached' plasma, charged particles are neutralized primarily on the limiter and the source of neutrals is strongly localized in the poloidal or toroidal directions. This does not allow one to properly take into account the CX effect in a one-dimensional model. Qualitative

estimations show (Tokar' 1992, 1993) that under conditions of plasma homogeneity on magnetic surfaces the influence of hydrogen neutrals, coming from the limiter, is not of principal importance for integral radiation losses.

After detachment, the *e*-folding length of the plasma density in the SOL increases and more charged particles hit the wall (Samm *et al* 1987). Therefore, the source of neutrals is delocalized over the whole LCMS and they may play a more important role in the behaviour of impurities.

Radiating impurity ions. In order to analyse the effect of CX on radiation losses, calculations have been done for the conditions corresponding to the onset of detachment. Figure 15 represents the profiles of power density of impurity radiation calculated for $\gamma_{rad} \approx 0.66$ ($I_p = 340$ kA, $a_C = 0.03$, $a_O = 0.01$). The dashed curve has been found for $n_e = 3.6 \times 10^{13}$ cm^{-3} without taking into account CX, the solid one for $n_e = 3.3 \times 10^{13}$ cm^{-3} with inclusion of the CX effect under the assumption that the influx of hydrogen neutrals is distributed homogeneously over the LCMS. The rate coefficients of CX are calculated according to Phaneuf *et al* (1987).

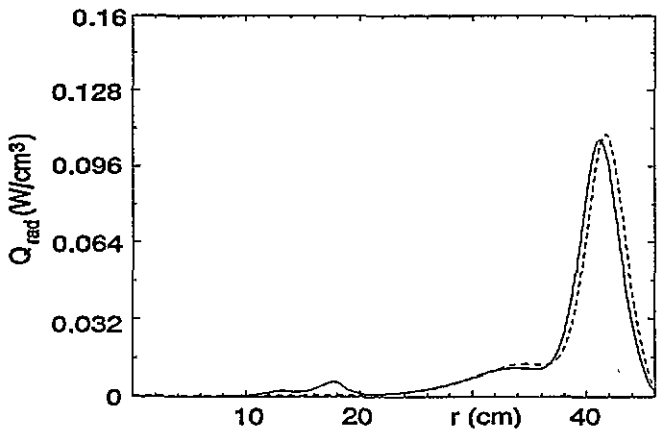

Figure 15. The profiles of the power density of radiation calculated without (dashed line) and with (solid line) taking into account of charge-exchange of impurities with hydrogen neutrals.

CX results in a slight increase in radiation losses (less than 10%). The cause of such a weak effect becomes understandable from the following qualitative consideration. The increase δn_3 of the density of the Li-like carbon ions due to CX does not exceed the value for which this source is balanced by the corresponding change of the sink due to ionization:

$$k_c^4 n_a n_4 \approx k_i^3 n_e \delta n_3$$

where k_c^z is the rate coefficient of CX, n_a is the neutral density. The magnitudes of parameters are taken corresponding to $\bar{n}_e = 3.8 \times 10^{13}$ cm^{-3}. According to figures 2, 3, 5 and 6, $T_{ei} \approx 60$ eV, $n_e \approx 2 \times 10^{13}$ cm^{-3}, $n_4 \approx 2 \times 10^{11}$ cm^{-3} and $n_a \approx 5 \times 10^9$ cm^{-3} in the region of the C^{+4} density maximum; for the rate coefficients one has $k_i^3 \approx 7 \times 10^{-10}$ and $k_c^4 \approx 3 \times 10^{-8}$ cm^3 s^{-1}. As a result, $\delta n_3 \approx 2 - 3 \times 10^9$ cm^{-3}, i.e. significantly less than the characteristic magnitude of n_3 found without taking CX into account (figure 3). This leads to a small increase of radiation.

Thus the calculations show a significantly weaker effect of CX on impurity radiation than was expected. The reason lies in that the role of CX is usually considered without taking

into account diffusion of the impurity. Both processes lead to an increase of the density of strongly radiating ions of low z, but the latter is more important. Moreover, in qualitative considerations the neutral density is taken as a parameter and its spatial variation is neglected. As a result, the effect of CX becomes stronger with increasing electron temperature. In a real plasma the temperature grows with the distance from the source of neutrals, i.e. it is accompanied by a decrease in n_a.

Impurity nuclei. For fully stripped ions, CX is already important at a low level of neutral density and, in particular, can compete with inward neo-classical convection (see previous section). In the plasma centre, where the impurity is in the plateau regime, the characteristic length of the change of n_i and T_i is of the order of the minor radius a. For the ratio of the divergence of the neo-classical particle flux and the sink of C^{+6} ions due to CX, one has the estimate

$$\left|\frac{1}{r}\frac{\partial(r\Gamma_{neo})}{\partial r}\right| / (k_c^z n_a n_z) \approx \frac{\rho_i^2}{a^2 z R n_a \sigma_c^z}.$$

Here $\sigma_c^z = k_c^z/(2T_i/m_i)^{1/2}$ is of 5×10^{-15} cm^2 for a typical ion temperature of 500–1000 eV in the plasma core.

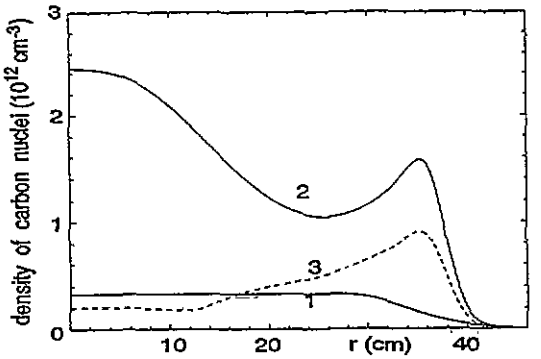

Figure 16. The profiles of C^{+6} density in a 'detached' plasma with $n_e = 3.8 \times 10^{13}$ cm^{-3} calculated in the diffusion approximation (1), with neo-classics (2) and with neo-classics and CX (3).

This ratio is less than 1 for n_a larger than 5×10^6 cm^{-3}, which falls in the range of neutral densities found in the plasma centre. Thus one should expect a strong effect of CX on the C^{+6} density. Figure 16 presents the profiles in a 'detached' plasma with $\tilde{n}_e = 3.8 \times 10^{13}$ cm^{-3} computed in the diffusive approximation ($V_\perp^z = 0$) without charge-exchange (1), with neo-classical convection without charge- exchange (2) and with neo-classical convection and CX (3).

We see that the inclusion of neo-classics without allowing for charge-exchange results in an unrealistically high density of carbon in the discharge. Such a level would lead to $z_{eff} \approx 3$, which is not observed in experiments. CX produces a strong sink of C^{+6} ions and reduces significantly their density in the plasma core. Although the density of ions of other z increases, the net effect is a reduction of the neo-classical contribution to the impurity transport owing to a drop in the mean impurity charge.

5. Conclusion

The radiation from light impurities at the plasma edge affects important processes in tokamak plasmas, such as the transport of energy, of background particles and of the impurity itself. In turn these processes influence the pattern and level of radiation. Therefore, a coherent approach is required for a proper consideration of plasma states with a high level of radiation like a 'detached plasma'.

In order to model such states the numerical code RITM (radiation from impurities in a transport model) has been developed; the results of computations for ohmic discharges are presented in the paper. They agree with experimental data in predicting the dependence of the radiation level on the averaged plasma density, discharge current, influx of impurities and transport coefficients, and correctly describe the conditions of detachment.

The time-dependent modelling of detachment provoked by an increase in the impurity release gives a characteristic time of detachment of 10–20 ms, in agreement with experimental observations. The importance of ohmic heating for the formation of a quasi-stationary 'detached' plasma is established: redistribution of the heat source with cooling of the edge prevents penetration of the radiating layer into the core. Modelling with a heat source whose density is independent of the plasma temperature shows a thermal collapse: the cooling wave is not slowing down and reaches the centre.

Neo-classical convection of impurity ions and their charge exchange with hydrogen neutrals are considered. It is shown that they are not of principal importance for ions of low charge, making the greatest contribution to radiation losses, and the diffusive approximation for simulations of detachment is justified.

At the same time, these processes influence significantly the density of fully stripped ions responsible for the plasma pollution, especially in a 'detached' plasma. The neo-classical transport tends to accumulate impurities in the plasma centre. Without charge exchange, an effective plasma charge could reach a value of 3, which is not observed experimentally. Due to the large cross section of charge exchange, this impurity sink suppresses this accumulation, in spite of the low density of hydrogen neutrals in the plasma core.

We expect to develop the model introducing an MHD consideration, to describe more realistically the current evolution and also to treat the cases with current disruption, taking into account recent developments in the transport theory and coupling the code RITM with a self-consistent description of the SOL plasma.

Acknowledgments

The author cordially thanks U Samm, H A Claassen, H Gerhauser and B Unterberg for very helpful discussions of the manuscript.

Appendix 1. Diffusion approximation for neutrals.

Main neutrals. Recombination of charged particles on the wall and gas puffing are the main sources of neutrals in tokamaks. Entering the plasma, they interact with electrons and ions; the model takes into account the following elementary processes. Molecules are dissociated and ionized by electrons and charge exchange with ions; in the first case two Franck–Condon atoms with an energy of $E_{fc} \approx 3$ eV are generated:

$$H_2 + e \rightarrow (k_d^m) \rightarrow 2H + e.$$

Molecule ions, produced in the second and third processes, are dissociated on ion and atom of the same energy:

$$H_2 + e \to (k_i^m) \to [H_2^+ + 2e] \to H + H^+ + 2e$$
$$H_2 + H^+ \to (k_c^m) \to [H_2^+ + H] \to 2H + H^+.$$

Atoms charge-exchange with ions,

$$H + H^+ \to (k_c^a) \to H^+ + H$$

are ionized by electrons,

$$H + e \to (k_i^a) \to H^+ + 2e$$

and are reproduced by recombination of ions and electrons:

$$H^+ + e \to (k_r) \to H.$$

In the bracket the notations used henceforth for the rate coefficients are given.

The behaviour of neutral particles in the plasma is described by the following set of kinetic equations averaged over magnetic surfaces:

molecules and reflected atoms

$$\frac{1}{r}\frac{d}{dr}(r v_r f_{m,ref}) = -\omega_{m,a} f_{m,ref} \tag{A1}$$

Franck–Condon atoms born by dissociation of molecules and molecule ions

$$\frac{1}{r}\frac{d}{dr}(r v_r f_{fc}) = -\omega_a f_{fc} + S_{fc}\varphi_{fc}(v_r) \tag{A2}$$

hot atoms produced by charge-exchange and recombination

$$\frac{1}{r}\frac{d}{dr}(r v_r f_*) = -\omega_a f_* + (k_c^a n_i n_* + S_*)\varphi_i(v_r). \tag{A3}$$

In these equations $f_{j=m,ref,fc,*}$ are distribution functions over the velocity component along the minor radius,

$$\omega_m = (k_i^m + k_d^m)n_e + k_c^m n_i \qquad \omega_a = k_c^a n_i + \omega_i \qquad \omega_i = k_i^a n_e$$

are the frequencies of disintegration of molecules and atoms in collisions with charged particles,

$$S_{fc} = [(k_i^m + 2k_d^m)n_e + k_c^m n_i]n_m$$

is the density of the source of Franck–Condon atoms; a two-velocity approximation is taken for their original distribution:

$$\varphi_{fc} = \frac{1}{2}[\delta(v_r - v_{fc}) + \delta(v_r + v_{fc})]$$

with $v_{fc} = (2E_{fc}/3m_a)^{1/2}$

$$S_* = [k_c^a(n_{fc} + n_{ref}) + k_c^m n_m + k_r n_e]n_i$$

is the source density of hot atoms which appear with the ion distribution φ_i; n_m, n_{ref}, n_{fc} and n_* are the densities of molecules, reflected, Franck-Condon and hot atoms, respectively.

The sources of molecules and reflected atoms are located at the LCMS ($r = a$) and originally these particles have velocities directed toward the discharge centre. But there are also particles which pass though the axis and move toward the LCMS. The existence of such particles among Franck–Condon and hot atoms is already caused by the position of their sources. Therefore it is natural to look for solutions to equations (A.1)–(A.3) in the form

$$f_j = A_+(r)\delta(v_r - v_j) + A_-(r)\delta(v_r + v_j). \tag{A4}$$

Here v_j are characteristic velocities: $v_m = (T_w/m_m)^{1/2}$ for molecules, where T_w is the wall temperature; $v_{ref} = (2E_{ref}/3m_a)^{1/2}$ for reflected atoms, where $E_{ref} = E_i R_E/R_P$, E_i is the energy of ions impinging the limiter and R_P and R_E are the coefficients of particle and energy reflection; $v_* = (T_*/m_a)^{\|}$ for hot atoms, where the temperature T_* has to be determined from the model.

Integrating equations (A.1)–(A.3) with f_j in the form (A.4) and with weights 1 and v_r one finds the equations for the particle and flux densities $n_j \equiv A_+ + A_-$ and $J_j = v_j(A_+ - A_-)$. Combining them appropriately we have obtained equations of a diffusive type for n_j. In the case of molecules

$$\frac{d^2 n_m}{dr^2} + \frac{dn_m}{dr}\left(\frac{2}{r} - \frac{1}{\omega_m}\frac{d\omega_m}{dr}\right) - n_m\left(\frac{\omega_m^2}{v_m^2} + \frac{1}{r\omega_m}\frac{d\omega_m}{dr}\right) = 0. \tag{A5}$$

To get an equation for the density of reflected particles one has to replace n_m by n_{ref}, w_m by w_a and v_m by v_{ref}, respectively. In the case of Franck–Condon atoms, besides analogous substitutions, the term $-w_a S_{fc}/v_{fc}^2$ has to be placed on the right. The particle and flux densities are related as follows:

$$J_{(j=m,ref,fc)} = -D_j\left(\frac{n_j}{r} + \frac{dn_j}{dr}\right)$$

with the diffusion coefficients $D_m = v_m^2/w_m$ and $D_{j=ref,fc} = v_j^2/w_a$.

For hot atoms an analogous procedure gives the equation for the pressure $P_* = n_* T_*$:

$$\frac{d^2 P_*}{dr^2} + \frac{dP_*}{dr}\left(\frac{2}{r} - \frac{1}{\omega_a}\frac{d\omega_a}{dr}\right) - P_*\left(\frac{\omega_a\omega_i}{v_*^2} + \frac{1}{r\omega_a}\frac{d\omega_a}{dr}\right) = -\omega_a S_* m_a \tag{A6}$$

and the flux density is determined according to the relationship

$$J_* = -\frac{D_*}{T_*}\left(\frac{P_*}{r} + \frac{dP_*}{dr}\right)$$

where $D_* = v_*^2/w_a$.

The boundary conditions of equations (A.5), (A.6) at the discharge axis ($r = 0$) follow from the reduction of the particle fluxes to zero. At the LCMS the fluxes of reflected atoms and molecules are related to the outflow of ions, Franck–Condon and hot atoms from the

plasma. It is assumed in the present paper that the SOL is transparent for all neutrals. In this case:

$$J_{\rm ref}(a) = -R_P(E_{\rm i})\Gamma^{\rm i}_{\perp}(a)$$

$$J_{\rm m}(a) = -\frac{1-R_P(E_{\rm i})}{2}\Gamma^{\rm i}_{\perp}(a) - \frac{R_{\rm rec}}{2}[J_{\rm fc}(a) + J_*(a)] - \Phi_{\rm gas}.$$

Here $R_{\rm rec}$ is the recycling coefficient and $\Phi_{\rm gas}$ is the density of the molecule influx due to gas puffing.

Reflection of Franck–Condon and hot atoms does not lead to a strong change of their mean velocity. Indeed, the velocity $v_{\rm ref}$ of reflected particles is related to the velocity $v_{\rm im}$ of the impinging ones as $v_{\rm ref} = v_{\rm im}(R_E/R_P)^{1/2}$. In the case of deuterium projectiles and a carbon wall, $0.8 < v_{\rm ref}/v_{\rm im} < 1$ for energies of projectiles less than 100 eV; $v_{\rm ref}$ becomes still closer to $v_{\rm im}$ for lower energies and heavier targets. Therefore, for these particles we assume that $v_{\rm ref} = v_{\rm im}$ and use R_E instead of R_P to describe correctly the transmission of the energy to the wall. Thus $A_-(a) = R_E A_+(a)$ or

$$J_j(a) = n_j(a)v_j\frac{1-R_E(E_j)}{1+R_E(E_j)}.$$

for $j =$ fc and $*$.

In order to find an equations to the temperature T_* of hot atoms equation (A.3) is integrated with the weight $m_{\rm a}(v_r^2 + v_\perp^2)/2$ and under the assumption that the distribution over the velocity component $v_\perp$, perpendicular to v_r, is a Maxwellian one. The result can be written as

$$\frac{{\rm d}T_*}{{\rm d}r} = \frac{k^a_{\rm c} n_{\rm i} n_* + S_*}{J_*}(T_{\rm i} - T_*). \tag{A7}$$

There is not *a priori* any boundary condition to this equation. But a condition sufficient for its solution follows from the structure itself. The source of hot neutrals is located inside the plasma and they move both towards the LCMS and towards the plasma centre. Therefore J_* changes sign at a certain point $r = r_*$ and $T_*(r_*)$ has to be equal to $T_{\rm i}(r_*)$ for continuity of $T_*(r)$. Physically this means that hot neutrals reside at r_* an infinite time and come into thermal equilibrium with ions. In order to find T_* in the vicinity of r_* the RHS of equation (A.7) is expanded into a Taylor's series.

The interaction between charged and neutral particles produces the source of main ions:

$$S_{\rm i} = (k^a_{\rm i} n_a + k^{\rm m}_{\rm i} n_{\rm m} - k_r n_{\rm i}) n_{\rm e} \tag{A8}$$

and sinks of energy from the plasma components:

$$Q_{\rm e,n} = -n_{\rm e}[E^a_{\rm i} k^a_{\rm i} n_a + (E^{\rm m}_{\rm i} + 2E_{\rm fc})k^{\rm m}_{\rm i} n_{\rm m} + \tfrac{3}{2}T_{\rm e}k_r n_{\rm i}] \tag{A9}$$

$$Q_{\rm i,n} = -\frac{3}{2}T_{\rm i}n_{\rm i}(k_r n_{\rm e} + k^{\rm m}_{\rm c} n_{\rm m} + k^a_{\rm c} n_a) + (E_{\rm ref} n_{\rm ref} + E_{\rm fc} n_{\rm fc} + \frac{3}{2}T_* n_*)(k^a_{\rm i} n_{\rm e} + k^a_{\rm c} n_{\rm i}) + E_{\rm fc} n_{\rm m}(k^{\rm m}_{\rm i} n_{\rm e} + k^{\rm m}_{\rm c} n_{\rm i}) \tag{A10}$$

where $n_{\rm a} = n_{\rm ref} + n_{\rm fc} + n_*$.

Table A1.

Species	E, eV	A, $eV^{1/2}$ cm^3s^{-1}	B, $eV^{-1/2}$	C, eV^{-1}
C^+	7.76	5.6×10^{-7}	0.213	0.0143
C^{2+}	7.59	7.27×10^{-7}	0.265	0.023
C^{3+}	5.48	7.54×10^{-7}	0.483	0.0565
C^{4+}	257	2.23×10^{-8}	0	0.0034
C^{5+}	250	4.63×10^{-9}	0	0.00058
O^+	6.23	1.04×10^{-7}	0	0.025
O^{2+}	7.94	1.59×10^{-7}	0	0.0282
O^{3+}	7.61	1.41×10^{-7}	0	0.0095
O^{4+}	9.7	2.7×10^{-7}	0	0.0143
O^{5+}	4.13	1.05×10^{-7}	0.2	0.0134
O^{6+}	400	6.17×10^{-9}	0	0.000362
O^{7+}	420	2.38×10^{-9}	0	0.000321

The reflection coefficients R_{PE} are estimated according to the formulae proposed by Behrisch and Eckstein (1986); the variation of the energy loss E_i^a on ionization of one atom with electron density and temperature (Janev *et al* 1984) is approximated by the formula:

$$E_i^a = (35 - 21.4e^{-n_1/n_e}) \exp\left[\frac{5.45}{T_e} e^{-(n_e/n_2)^{0.26}}\right]$$

where T_e, E_i^a in eV, $n_1 = 5 \times 10^{13}$ cm^{-3} and $n_2 = 1.37 \times 10^{14}$ cm^{-3}; for molecules $E_i^m \approx 15.6$ eV.

Atoms of impurities are ionized in the plasma and reproduced by recombination of singly charged ions and electrons. Equations for their densities are analogous to equations (A.5) and (A.6).

Appendix 2. The power density of ohmic heating

$Q_{e,h}$ is determined by the longitudinal electric field $E_\parallel$ and current density $j_\parallel$:

$$Q_{e,h} = \sigma_\parallel E_\parallel^2.$$

The electrical conductivity $\sigma_\parallel$ is calculated according to the formula (Anders 1990)

$$\sigma_\parallel = \sigma_{cl} \frac{1 + 2.96 z_{eff} + 0.753 z_{eff}^2}{1 + 1.19 z_{eff} + 0.222 z_{eff}^2} f_{neo}$$

where $\sigma_{cl} = n_e e^2 t_e / m_e$ is the classical conductivity, z_{eff} is the effective plasma charge and the coefficient

$$f_{neo} = \left(1 - \frac{f_T}{1 + \xi \varepsilon^{-3/2}/g_e}\right) \cdot \left(1 - \frac{c_R f_T}{1 + \xi \varepsilon^{-3/2}/g_e}\right)$$

with

$$f_T = 1 - \frac{(1-\varepsilon)^2}{\sqrt{1-\varepsilon^2}(1 + 1.46\sqrt{\varepsilon})} \qquad \xi = 0.58 + 0.2 z_{eff} \qquad c_R = \frac{0.56}{z_{eff}} \frac{3 - z_{eff}}{3 + z_{eff}}$$

$e = r/R$ and g_e being the electron collisionality, takes into account neo-classical effects.

The electric field is determined from a given value of the plasma current I_p. Finally

$$Q_{e,h} = \frac{\sigma_\parallel I_p^2}{4\pi^2} \left(\int_0^a \sigma_\parallel r \, dr\right)^{-2}.$$

Appendix 3. Energy losses from electrons due to collisions with impurities

The power density of this channel of the energy losses is as follows:

$$Q_{e,I} = \sum_z (k_i^z I_z + \frac{3}{2} T_e k_r^z + B_z z^2 \sqrt{T_e} + L_z) n_z n_e.$$

The first term is due to ionization, the second one is due to recombination of ions and electrons, the third one is due to bremsstrahlung; the ionization potentials I_z and the rate coefficients k_i^z are taken from Bell *et al* (1982), the coefficients k_r^z, B_z are calculated according to formulae of Post *et al* (1977).

The last term in $Q_{e,I}$ corresponds to the line radiation of impurities and is of most importance for the plasma edge:

$$L_z = \sum_{i,j} k_{i,j} E_{i,j}.$$

Here k_{ij} is the rate coefficient of excitation on the level j from the level i and $E_{i,j}$ is the excitation energy. For plasmas of interest of not too high densities, transitions from the ground state are of maximum importance and the total energy spent on the excitation is lost from the plasma because de-exciting collisions with electrons are too rare.

The information on k_{ij} and $E_{i,j}$ is taken from Itikawa *et al* (1985) and the temperature dependence of the cooling rates L_z is approximated by the formula (Tokar' 1992):

$$L_z = \frac{A\sqrt{T_e}}{1 + B\sqrt{T_e} + CT_e} \exp(-E/T_e).$$

The 'activation' energies E and coefficients A, B, C are presented in table A1.

Making use of the foregoing formula reduces dramatically the time spent on computation of radiation losses.

References

Abramov V A, Lisitsa V S and Morosov D Kh 1992 *Contrib. Plasma Phys.* **32** 400

Allen S L *et al* 1981 *Nucl. Fusion* **21** 251

Anders A 1990 *A Formulary for Plasma Physics* (Berlin: Akademie)

Ashby D E T F and Hughes H M 1981 *Nucl. Fusion* **21** 911

Behrisch R and Eckstein W 1986 *Physics of Plasma-Wall Interaction in Controlled Fusion* ed D E Post and R Behrisch (New York: Plenum) p 413

Bell K L *et al* 1982 Atomic and molecular data for fusion (part 1) *Culham Laboratory Report* CLM-R216

Behringer K H *et al* 1986 *Nucl. Fusion* **26** 751

Bogen P and Rusbüldt D 1992 *Nucl. Fusion* **32** 1057

Brau K *et al* 1983 *Nucl. Fusion* **23** 1657

Burrell K H 1976 *Phys. Fluids* **19** 401

Castracane J. *et al* 1987 *Nucl. Fusion* **27** 1921

Claassen H A *et al* 1990 *J. Nucl. Mater.* **176–177** 398

Claassen H A and Gerhauser H 1992 Impurity transport at the plasma edge: the transition from 2D to 1D Models *Institut für Plasmaphysik Report* Jül-2576

Dnestrovskij Yu N *et al* 1979 *Plasma Phys. Controlled Nucl. Fusion Res.* (Vienna: IAEA) vol 1 p 443

Gerhauser H and Claassen H A 1993 *Proc. 20th European Conf. on Controlled Fusion and Plasma Physics (Lisboa: European Physical Society)* vol 17C-2 p 835

Greenwald M *et al* 1988 *Nucl. Fusion* **28** 2199

Groebner R J *et al* 1990 *Phys. Rev. Lett.* **64** 3015
Hiroe S *et al* 1992 *Nucl. Fusion* **32** 1107
Hinton F L and Hazeltine R D 1976 *Rev. Mod. Phys.* **48** 239
Hintz E 1992 *Contrib. Plasma Phys.* **32** 422
Ida K *et al* 1994 *Phys. Plasmas* **1** 116
Itikawa Y *et al* 1985 *Atomic Data and Nuclear Data Tables* **33** 150
Janev R K *et al* 1984 *J. Nucl. Mater.* **121** 10
Krasheninnikov S I 1988 *Sov.–JETP Lett.* **5** 287
Lipschultz B 1987 *J. Nucl. Mater.* **145–147** 15
McCracken G M *et al* 1987 *J. Nucl. Mater* **145–147** 181
Neuhauser J *et al* 1986 *Nucl. Fusion* **26** 1679
Ohyabu N 1979 *Nucl. Fusion* **9** 1491
Phaneuf R A *et al* 1987 Collisions of carbon and oxygen ions with electrons, H, H_2 and He *Oak Ridge National Laboratory Report* ORNL-6090/V5
Post D E *et al* 1977 *Atomic Data and Nuclear Data Tables* **20** 397
Rebut P H and Green B J 1977 *Plasma Phys. Controlled Nucl. Fusion Res.* (Vienna: IAEA) vol 2 p 3
Rogister A 1994 *Phys. Plasmas* **1** 619
Samm U *et al* 1987 Properties of 'detached' plasmas *Institut für Plasmaphysik Report* Jül-2123
Samm U *et al* 1989a *J. Nucl. Mater.* **162–164** 24
Samm U *et al* 1989b *Proc. 16th European Conf. on Controlled Fusion and Plasma Physics (Venice: European Physical Society)* vol 13B-3 p 991
Samm U 1990 Radiation control in a limiter tokamak *Institut für Plasmaphysik Report* Jül-2378
Samm U *et al* 1990 *J. Nucl. Mater.* **176–177** 273
Samm U *et al* 1992a *J. Nucl. Mater.* **196–198** 633
Samm U *et al* 1992b *Plasma Phys. Controlled Nucl. Fusion Res. (Vienna: IAEA)* Vol 1 p 309
Samm U *et al* 1993 *Plasma Phys. Control. Fusion* **35** B167
Schorn R P *et al* 1991 *Appl. Phys.* B **52** 1991
Stacey W M 1987 *Nucl. Fusion* **27** 1213
Stacey W M 1993 *Pfys. Fluids* B **5** 1413
Stangeby P C and McCracken G M 1990 *Nucl. Fusion* **30** 1225
Strachan J D *et al* 1982 *Nucl. Fusion* **22** 1145
Strachan J D *et al* 1987 *J. Nucl. Mater.* **145–147** 186
Tokar' M Z 1988 *Contrib. Plasma Phys.* **48** 355
Tokar' M Z 1989 *Proc. 16th European Conf. on Controlled Fusion and Plasma Physics (Venice: European Physical Society)* vol 13B-3 p 1035
Tokar' M Z 1992 One dimensional model of a tokamak edge plasma under conditions of strong impurity radiation *Institut für Plasmaphysik Report* Jül-2588
Tokar' M Z 1993 *Plasma Phys. Control. Fusion* **35** 1119
Tokar' M Z 1994 *Nucl. Fusion* **34** 853
Ulrickson M, The JET Team and The TFTR Team 1990 *J. Nucl. Mater.* **176–177** 44
Unterberg B *et al* 1993 *Proc. 20th European Conf. on Controlled Fusion and Plasma Physics (Lisboa:European Physical Society)* vol 17C-2 p 663
Vallet J C *et al* 1991 *Phys. Rev. Lett.* **67** 2662
Van Nieuwenhove R *et al* 1992 Proc. *IAEA Tech. Comm. Meet. on Tokamak Plasma Biasing (Varennes)* p 48
Wenzel K W and Sigmar D J 1990 *Nucl. Fusion* **30** 1117
Weynants R R *et al* 1988 Plasma confinement in attached and detached limiter tokamak plasmas *Laboratoire de Physique des Plasmas Report* H-PWW-88
Yamagishi T *et al* 1983 *Nucl. Fusion* **23** 189